Marine measurement and real-time control systems' applications

Melek Ertogan[a,c,1], Seniz Ertugrul[b] , Philip A. Wilson[c], Gokhan Tansel Tayyar[d],

[a] Maritime Faculty-Marine Engineering, Istanbul Technical University, Turkey

[b] Mechanical Engineering, Istanbul Technical University, Turkey

[c] Faculty of Engineering and the Environment, University of Southampton, U.K.

[d] Naval Architecture and Marine Engineering, Istanbul Technical University, Turkey

Abstract

Measurement, data transfer, modelling, controller systems are main subjects of interdisciplinary area during prototyping of marine automatic control systems. Experimental parameter identification under changing environmental conditions is an essential step for modelling and control system design are in question for various marine applications. The selection of variables to be measured, type of measurement sensors, type of control algorithms and controller systems, communication, signal conditioning are all important topics for parameter identification and real-time control applications in maritime engineering. The objective of this paper is to present brief review these important topics based on our case studies, such as ship roll motion reduction control, optimal trim control of a high speed craft, and dynamic position control of underwater vehicles. These projects involved extensive dynamic modelling, simulation, control algorithm design, real-time implementation and full-scale sea trials. In this paper, presented the methods, and the required characteristics of the marine control systems are proved with the results obtained by the simulation and test studies. Also, insight into the selection of hardware and software components for mechatronic applications in marine engineering is provided.

Keywords: Marine vehicles' motions, measurement, system identification (SI), prototyping, real-time control, full-scale experiments

1. Introduction

[1] Corresponding author at: Marine Engineering Faculty, Istanbul Technical University, Tuzla, Istanbul, Turkey.
Phone: +90-533-3408113
E-mail addresses: ertogan@ itu.edu.tr , melekertogan@gmail.com (M. Ertogan),
seniz@itu.edu.tr (S. Ertugrul), Philip.Wilson@soton.ac.uk (P.A. Wilson),
tayyargo@itu.edu.tr (G.T. Tayyar),

Automatic control systems' applications in marine engineering include many differences, compared to other engineering controller systems. It is important to identify the features of sensors, communication type, control algorithm type, and controller systems for measurement, and real-time control processes according to an application area in the maritime industry. Measurement, signal processing, communication, modelling, and prototyping for marine vehicles' control systems were reviewed respectively in the following subsections.

1.1 Marine vehicles' motion and position measurement

Determination of sensors for marine vehicles' motion and position measurement depends on application areas such as sea surface and underwater vehicles. In addition to these, tank and open sea test types are other criterions to identify the sensors.

1.1.1 Sea surface vehicles' motion and position measurement

Sensors are used as feedback signals in closed-loop controller systems, and/or to check manually in open control systems. Global Positioning System (GPS), gyroscopes, Inertial Measurement Unit (IMU), Attitude and Heading Reference System (AHRS), a ship's speed measurement relative to the water, wind direction, wind speed, echo sounder, etc. are utilized in the maritime industry.

Accuracy, resolution, bandwidth, etc. features of a sensor must be evaluated while choosing according to system requirements. The system requirements are such as a system's response time, a closed-loop controller time, sample time and error tolerance value. A high-performance sensor should have a fast response time, stable output, and without noise signals.

IMU sensors are used for measuring ship motions, linear acceleration, angular rate, and angular position. Low drift, and high reliability features of an IMU sensor must be considered. Numerical integration causes the drift of IMU sensor. There are many low price IMU sensors in industry, but they have high drift during long run hours. The high reliability feature of an IMU shows that it can be run over a long period, for instance >20000 hours.

There are two types of IMU sensors. The first type of IMU consists of accelerometers and gyroscopes. Typically, each sensor has from two to three degrees of freedom defined for x, y, and z axis. Combining both sensors will total up four to six degrees of freedom (DOF). Angles (pitch, roll) can be measured from both sensors, so both data can be calibrated to get more accurate data. Yaw angle can only be measured by a gyroscope. The advantage of this type IMU is that it will not be affected by external magnetic fields. However, depending on two type of sensors may not be enough to increase the accuracy of output data, due to the sensors' noise, and the drift of the gyroscope. The second type of IMU consists of an accelerometer, gyroscope, and magnetometer to obtain measurements in three different axes, making a

total of 9 DOF. The magnetometer is used to measure yaw angle rotation, so yaw angle can be calibrated by both a gyroscope, and a magnetometer (Ahmed, et al., 2013).

The key difference between IMU and AHRS is that an AHRS has the addition of on-board processing system. Non-linear estimation such as an Extended Kalman Filter is typically used to calculate attitude and heading information. GPS provides global position of x- and y-axes, and relative speed of a ship. However, it gives about 2-3 s delayed result, and its nominal accuracy is 5-10 m. Differential Global Positioning System (DGPS) uses a network of fixed ground based stations, so its nominal accuracy is improved about 5-10 cm, but it can be used only the coast areas.

A ship's speed measurement before GPS is important to the navigation system. Dead reckoning position calculation depends on a ship's heading and speed. A ship's speed can be measured relative to either the seabed or to the water flowing past the hull (water reference speed). The speed logging methods are the pressure tube log, electromagnetic log, and Doppler speed log (Tetley and Calcutt, 2001).

1.1.2 Underwater vehicles' localization system

Localization and dynamic position control of Autonomous Underwater Vehicles (AUVs) are very important subjects while AUVs are operated as hover style and flight style such as path following, target tracking control applications for underwater construction, maintanence, also underwater mapping. Other important subject, energy efficiency can be obtained by using succesfull localization and dynamic position control because of preventing drifts.

Data fusion of sensors for navigation was studied extensively in the literature, because localization of AUVs is ongoing problem. The most common underwater navigation includes Doppler Velocity Log Sensors (DVL), Ultra Short Baseline (USBL)/Long Baseline (LBL) with IMU. The integration of DVL/IMU for underwater vehicle was studied in (Chong-Moo Lee, et al., 2005) using multisensor Kalman Filtering. DVL-based navigation causes the drift in the position estimate, and this even more difficult in long-range AUV navigation more than 300m. So, a DVL is hardly used alone for underwater navigation, it is combined with other sensors for example acoustic sensors (Bandara et al., 2016). USBL and LBL-based navigation systems of AUVs are explained comperatively, and indicated drawbacks of USBL during ice are docking (Plueddemann et al., 2012).

Localization of AUVs was calculated online based on Kalman Filtering by using IMU and laser-based vision system. These experimental studies were applied in a tank, but measurement range by using laser-based vision feedback was very short distance such as from 30cm to 5m, and computer vision feedback was carried out at low frequency (Karras, et al., 2011; Cain and Leonessa, 2012).

USBL/LBL acoustic position measurement system doesn't work correctly for localization of AUVs in the tank tests such as control algorithm verifying purpose, because of wall effects. Also, range of localization of AUV by using vision feedback is very short and vision feedback frequency is very low. Dead reckoning method including DVL/IMU may cause drifts of AUV motion. Consequently, integration of 2 or 3-echosounding altimeters to IMU and pressure depth sensor on AUV can be used to localize of AUV in the tank tests. 2-echosounding altimeters adding on AUV enables to measure positions of X-, and Y-axes, so localization of AUV can be obtained Fig. 1.a. Frequency range of an altimeter is 1-4 Hz, and distance range feedback of it is 5-100 m. if a magnotometer has big drifts during the tank tests, 3-echosounding altimeter can be used to measure yaw angle, as well Fig. 1.b. Also, an echosounding altimeter has lower price than DVL.

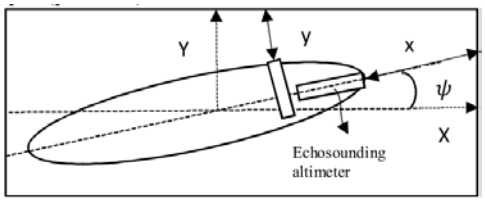

Fig. 1.a. 2-echosounding altimeter integrating to AUV localization.

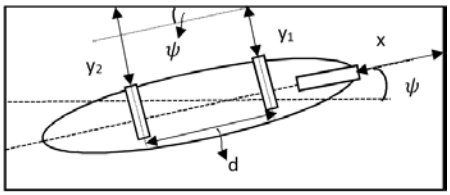

Fig. 1.b. 3-echosounding altimeter integrating to AUV localization.

In addition to these, an echosounding altimeter would be used to keep distance control on AUVs in real environment areas for example during flight style operation of AUVs in shallow coastal and under ice areas, also during docking of AUVs, because USBL measurement system may not work correctly near shore. These would be provided collision avoidence of AUVs from fix and dynamic targets.

1.2. Noise, derivative problems, and filtering methods

In real-time, closed-loop control applications, there are problems such as noisy measurements and derivative processes. A variety of filtering methods are available to make noisy measurements smooth in the literature. A simple filtering method is that noisy measurement may be filtered by averaging the sampled data. Butterworth filters are frequency based digital filters. They include cut-off frequency, low-pass, high-pass, band-pass, etc. The common problem encountered in using Butterworth filters is the phase delay problem (Butterworth, 1930).

Furthermore, Kalman filter is widely used in time series for signal processing. Complementary filtering (CF) may be another method to be obtained accurate and stable data from an AHRS based on low-cost MEMS (microelectromechanical systems) provided that high frequency such as 100 Hz is applied (Wang, et al., 2014).

The Kalman filter is applied not only in signal processing but also in the estimation of velocity. However, Kalman filter is a model-based approach that requires the target velocity trajectory, so it cannot be applied to the case where arbitrary

velocity is measured. The derivation of position signal data may be needed because of reducing feedback signals, or not having an alternative sensor for measuring velocity. A general derivative process is the Euler method, but this method may not give accurate results. An efficient velocity estimation algorithm is Enhanced Differentiator (ED) (Su, et al., 2006).

1.3. Data transfer and communication types

The sensors feature different means of communication such as analog, RS232/RS485, usb, NMEA 0183/ 2000, ethernet etc. Although most of these communication types are the same as general engineering applications, NMEA is a specific protocol for the maritime industry. A digital signal is preferred to an analog signal, because an analog signal has a disadvantage for long distances during transferring data between a controller and feedback signals. Data transfer time of a common communication must be enough for sampling time, and closed loop time of a real-time application.

Communication systems in a maritime application are CANopen (CAN), NMEA, MODBUS, PROFIBUS, PROFINET, Ethernet TCP/IP, EtherCAT protocols. The maritime automation systems can be very complex, it is generally structured into three hierarchical levels such as field-level networks, control-level networks, and information-level networks (Bachmann, 2015).

The field-level communication includes sensors, and actuators. The task of the field-level communication is to transfer data between sensors, actuators, and the technical process. The data can be digital, analogue, or serial. The serial communications are RS232, RS422, RS485. Those are point-to-point communication methods. Field level networks are a variable category. Choosing the right network depends on a variety of specifications such as message size, response time, etc. In maritime industry, the fieldbus networks are CANopen, NMEA0183/2000 (Djiev, 2015).

The control level networks are used between controllers such as Programming Logic Controllers (PLCs). Also, they are preferred for distributed control systems (DCS), and Human Machine Interface (HMI) units. The control level networks are MODBUS, PROFIBUS, PROFINET, Ethernet TCP/IP, EtherCAT. The information level is the top level of a maritime automation system. The information level network gathers the management information, and manages the whole automation system. Ethernet networks connects other maritime networks.

A speed of a CAN network is up to 1 Mbit/sec. Its average message takes 130 µsec per node. A CAN network supports up to 128 nodes. Its update rate is approximately 1 KHz. Cycle time range of CAN bus system is about 20-100 ms. The cycle time of data transfer in communication can be varied according to Input/Output (I/O) nodes. RS232 serial communication is an economical single-axis solution. Its total message time is up to 1.3 ms. RS232 messages can be longer than CAN, but it is much slower than a 1 Mbit/s CAN bus. RS485 serial communication can support multiple-

axis nodes up to 32. Its messages can be longer than CAN. Total message time and reply is 174 µsec. This is the same as a 1 Mbit/s CAN bus. NMEA 0183/2000 can be generally used for a GPS communication interface. Its update time is up to 10 Hz (Talbot and Ren, 2009; Servo2go, 2013). If NMEA 0183/2000 is used as communication interface for multiple nodes, its cycle time is min. 1 s.

PROFIBUS has certain protocol features that let certain versions of it operate in multi-master mode on RS-485, while MODBUS could be only single master. However, MODBUS can operate on Ethernet including multiple masters while PROFIBUS cannot operate on Ethernet. MODBUS is a very simple, easy-to-use protocol according to PROFIBUS, when it connects a controller to one smart device in a point-to-point configuration. However, MODBUS may have problems in multi-vendor applications. The transmission rate of MODBUS is up to 1 Mb/s. PROFIBUS network has up to 12 Mb/s transmission rate, and its cycle time is lower than 2 msec. PROFINET operating on Ethernet is different from PROFIBUS, and its transmission message capacity is a maximum of 100 Mb/s. The Ethernet network has approximately 10 Mbit/s, and a maximum 1 KHz update time. EtherCAT, a high-performance Ethernet-based network protocol has up to 200 Mbit/sec transmission rate. Its cycle times can reach less than 1 KHz (Knezic and Ivanovic, 2013).

1.4. Modelling of marine vehicles' dynamics for control applications

A nonlinear mathematical model of ship motions which have six degrees of freedom would be desired to design a controller. There are several modelling approaches available for simulation purposes. The selection of modelling approach might be the nonlinear modelling which is relatively complicated but may represent actual dynamics better. When structure of the model is readily available for the specific type of sample ship, coefficients may be determined by utilizing data collected by model tests or full-scale sea trials. Linearized models, such as transfer functions or state-space models, might be adequate for the initial control design. However simulation results may greatly differ from actual system responses.

Perez and Blanke reviewed the models for describing the motion of a ship in four degrees of freedom as surge, sway, roll, and yaw for control applications in their report. The nonlinear, and linearized state space hydrodynamic models of two ships as a container, and a naval vessel were presented in the report. The nonlinear hydrodynamic models were validated with full scale experiments. In conclusion, the nonlinear models were described the dynamic response of the ships more accurately than the linear models. However, the linear models performed well in the range of the natural frequency, but their behaviour departed from the nonlinear counter parts at low frequencies. Therefore, using models

fitted at different frequencies is proposed. In addition to this, some parameters are more sensitive than other parameters, so using these parameters in the linearized models is suggested in the report (Perez and Blanke, 2002).

Modelling methods of ship motions are white box modelling as fluid structure interaction methods based on Navier-Stokes equations, grey box modelling including a partial theoretical structure with experiment data, and black box modelling using only experiment data. Although white box modelling can promise reliable prediction of ship motions, this method isn't practical to use for control design purposes because of its time consuming. Grey and black box modelling studies are called as System Identification (SI) method in multidisciplinary area, and SI method has shown a good level accuracy according to empirical and theoretical methods (Ljung, 1999).

A ship roll motion mathematical model depending on pitch and heave motions was studied according to grey box method for a ship roll motion reduction control design (Ertogan, et al., 2016). Also, a hydraulic system for actuating ship stabilizer fin system was modelled according to grey box method, as well (Zihnioglu, et al., 2016). Furthermore, a coupled mathematical model for pitch-surge motions of a high speed craft was studied by using black box method (Ertogan, et al., 2017).

1.5. Marine mechatronic systems' prototyping and control

There are a variety of controller systems, such as analogue electronic card, microcontrollers, microprocessors, and embedded microprocessors such as PLCs, industrial PCs, for the maritime industry. Memory requirement, cycle time, a number of I/O nodes, I/O message transfer capacity and time, and communication options must be taken into account for a maritime application while identifying a controller type. A cost factor is another evaluation factor during choosing a controller. The controllers in marine equipment have to work continuously, 24 hours a day, 7 days a week, so they must not be interrupted. It would also be preferable to save the histories of their operations, so that the system can be diagnosed or debugged.

The actuator systems also have various options such as hydraulic, pneumatic, and electric systems. Space-saving, ease-of-operation and maintenance specifications should be taken into account during the selection of an actuator system. Tests of marine engineering controllers during the research process must be done because of the evaluation of systems' performances, and safety.

In addition to these, a marine equipment has to have maritime certifications as well as CE certificates. A chosen controller and an actuator must work in variable environmental conditions such as high temperature, air humidity, salt spray, etc., so they have to have high International Protection (IP) standards for marine applications. Both the

certification and IP standards must be taken into account while transition process from a prototype production to series production.

In the literature, there are less studies on marine mechatronic systems' prototyping than theoretical studies. Some of them are given as examples in this part. A remote controlled an in-scale fast-ferry model was constructed for autopilot design purpose (Valesco, et al., 2013). A torpedo-shaped, and fully-actuated underwater robotic vehicle (URV) prototype was developed to be performed environmental survey and surveillance task in range shallow water (Xianbo, et al., 2017). Also, a continuous control design method is proposed for the URV during transition between fully-actuated and under-actuated throughout changing speed profiles (Xianbo, et al., 2015). Furthermore, another fully actuated autonomous underwater vehicle (AUV) named as Delphin2 was developed at the University of Southampton to provide a test bed for research in marine robotics (Phillips, et al., 2009).

An ship roll motion reduction control system was set up, and an advanced controller was developed (Ertogan, et al., 2016). Then, a hydraulic and fin mechanic system for actuating ship stabilizer fin system prototype was developed and constructed, as well (Ertogan, et al., 2015; Zihnioglu, et al., 2016). Furthermore, a trim control system was installed on a high speed craft to improve an optimum trim controller (Ertogan, et al., 2015, 2017).

In this paper, mathematical modelling, and operations, measurement, and control of the applied marine mechatronic systems are briefly reviewed, after their setups are described in the next sections. Presented the methods, and the required characteristics of the control systems are proved with the results obtained by the simulation and test studies.

2. Applied mechatronic systems' setups

An advanced controller for a ship roll motion reduction fin system was designed in the first stage of the projects. An active stabilizer fin system actuated by a hydraulic system was installed on Marti. The specifications of the full-scale experimental setup are given in Section 2.1. A hydraulic and fin-shaft mechanic systems of a stabilizer active fin system was developed in the second stage of the projects. Furthermore, a fin – shaft system of a stabilizer fin system was produced. As a result of the studies, the prototype of the full active fin stabilizer system was assembled, and installed on Volcano 71. The specifications of the prototype are given in Section 2.2. In the recent finalized project, an optimal automatic trim control of a high-speed craft was studied. This control system was applied on an interceptor, and a trim tab systems. An interceptor, and a trim tab systems were installed on Volcano71 for sea trial tests. The specifications of the test apparatus for the trim control system are given in Section 2.3.

2.1 Ship roll motion reduction control system

The advanced controller of the ship roll motion reduction system was implemented on Marti a displacement-type ship owned by Istanbul Technical University. A hydraulically actuated fin stabilizer system was mounted on Marti, as shown in Fig. 2. The particulars of Marti are as follows: length overall L_{OA}=16.5 m, length on the waterline L_{WL}=15.5 m, moulded beam B_M=4.5 m, moulded depth D=2.29 m. Hydrostatic characteristics of the ship are displacement Δ=30.94 tons, draft T=1.36 m, natural period w_o=4 s, metacentric height $\overline{GM}$=0.5 m for mid-voyage load condition. The ship's engine power is 170 BHP, reaching a maximum speed of 9 knots. The propulsion system has a three bladed, 80 cm diameter propeller.

Fig. 2. Marti was launched after the installation of the fin stabilizer system.

The actuator system of the ship roll motion reduction system has a pair of hydrodynamic fiberglass fins, a hydraulic vane pump, and a pair of servo hydraulic valves and cylinders. The active fin stabilizer system's features are as follows: the fin surface area of $A_f = 0.232\ m^2$, the hydraulic working pressure of P=70 bars, the electric motor power of W=3 kW, A pair of proportional valves with a Linear Variable Differential Transformer (LVDT) type feedback sensor. A pair of analogue PID controlled driver circuits were used to provide servo control of the hydraulic system by using LVDT of a pair of proportional valves, and the fins' angular position feedback sensors.

A mobile workstation with a dual-core, 2.66 GHz processor, 32 bit operation system, and 4 GB RAM was used for laboratory work and sea trials. An industrial embedded microprocessor unit, UEISIM300^{TM} with Linux operating system, 400 Mhz & 32 bit processing unit, 128 MB RAM, 2 GB memory, and a 5 kHz update rate was used for data acquisition, data logging and real-time control. Data communication between the computer and I/O system was provided with RS232. Ethernet protocol was used to follow real-time processing on a PC. The I/O system of the industrial embedded microprocessor unit includes Analog Input (AI), Analog Output (AO), and Digital Input/Output

(DIO) boards. The ship's roll and pitch angles at maximum $\pm 75^{\circ}$ were measured using a dual-axis analog tilt sensor, Crossbow CXTA02^{TM} with a resolution of 0.05°.

2.2 Ship active roll motion reduction hydraulically actuated fin system

The prototype of the active fin stabilizer system was assembled and installed on Volcano 71, as shown in Fig. 3. Volcano 71 is a high speed craft. It has a deep V form. The other particulars of Volcano 71 are as follows: length overall L_{OA}=10.86 m, length on the waterline L_{WL}=9.4 m, beam B=3.3 m, depth D=1.15 m, deadrise angle $\beta = 16^{\circ}$. Hydrostatic characteristics of it are displacement Δ=5.351 tons, draft T=0.45 m, metacentric height $\overline{GM}$=0.64 m, natural period w_o=3 s for mid-voyage load condition. Its sterndrive engine power is 2x385 BHP reaching a maximum speed of 40 knots.

Fig. 3. The fin stabilizer system's prototype was assembled on Volcano 71.

A hydraulic system was assembled with a pair of asymmetric cylinders having a 20 cm^2 cap and 15 cm^2 rod side areas with 10 cm stroke, a pair of four-way, and three-position critically centred proportional valves. A pair of analogue PID controlled driver cards for servo controlled valves, a pair of five kΩ potentiometers for measuring the angular position of the fins were used. The hydraulic system also consists of 1 pressure compensated variable displacement pump, 1 pressure relief valve, filters, tank. The particulars of the variable displacement pump are a maximum pressure of P_{max}=90 bar, and a flow speed Q=10 lt/min. The fin surface area of the stabilizer fin system is A_f=0.18 m^2. The electric motor power of the hydraulic system is 1.5 kW. The assembly of the hydraulically actuated stabilizer active fin system installed on Volcano 71, and the hydraulic system of schema are shown in Fig. 4.a and 4.b respectively.

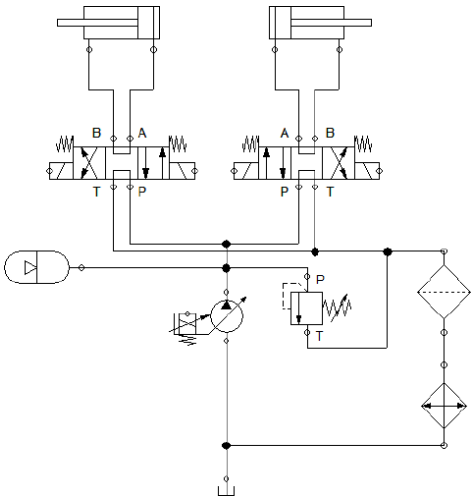

Fig. 4.a. The hydraulic system's installation on Volcano 71.

Fig. 4.b. The hydraulic system's scheme

A PLC, Allen-Bradley 1769-CompactLogix controller was used in this project, because it has a certificate, flexible programming, and a user interface panel. The controller with certificate was preferred, taking into consideration that the next stage in the series production status. It has 1 MB user memory, 1 GB secure digital memory card. Its cycle time is 1ms. It has a dual port ethernet communication. It has continuous, and periodic controller tasks. The programming languages of it are Ladder, Structured Text, and Function Block.

The I/O expansions of the PLC are digital input/output, and adjustable analog input/output modules. The analog input module has 8 input channels, differential or single-ended, 16 bit resolution, and input range selection for each channel such as 0-20, 4-20 mA, and 0-5, 1-5, 0-10, ±10 V. The analog output module has 4 output channels, single-ended, 14 bit resolution, and adjustable out range selection. In addition to the dual-axis analogue tilt sensor, a single axis analog gyroscope was used for measuring roll velocity values. The standard range full scale of the gyro is $\pm 90^{\circ}/s$.

2.3 Trim control system of a high speed craft

An optimum trim control of a high speed craft was studied in the recent finalized project. A pair of interceptor systems, and a pair of trim tab systems were installed on Volcano71 for the real-time applications, as shown in Fig. 5. The blade size and stroke of the interceptor are 430 mm, and 50 mm, respectively. The size of the trim tab's plate is 450 mm x 250 mm. The pulse width modulation (PWM) drivers were provided for the interceptor and trim tab systems.

The mobile computer and the industrial embedded microprocessor unit with I/O electronic cards were used for measurement and control. Their specifications are defined in Section 2.1. In addition to this, the serial module was added to the embedded controller.

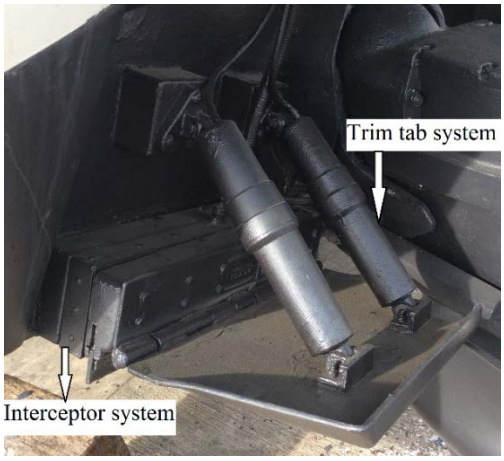

Fig. 5. An interceptor and a trim tab systems were mounted on Volcano 71

A GPS-aided inertial measurement unit (IMU), Microstrain 3DM-GX4-45^{TM} including triaxial accelerometer, gyroscope, magnetometer, was chosen because of its ability to measure a ship's dynamics, and speed. The measurement range of the IMU's outputs are ±5 g with 0.1 mg resolution, and $\pm 300^{\circ}/s$ with $0.008^{\circ}/s$ resolution. Its data output rate is 1 Hz to 500 Hz. Its GPS data output rate is 1 Hz to 4 Hz. The IMU's communication interface is RS232 protocol. The GPS-integrated IMU was used for modelling a ship's dynamics to design the controller. The GPS alone was provided for final prototype production. Its communication interface is NMEA 2000 protocol. Also, a pair of electronic sensors with NMEA 2000 network for measuring fuel flow was used. In addition to these, a multisensor with NMEA 2000 network was provided, and installed on the ship for measuring sea water flow velocity, depth.

3. Modelling and determination of parameters for control applications

A mathematical model of ship motions was studied according to grey box method for the ship roll motion reduction controller. Six degrees of freedom nonlinear ship dynamics under environmental and loading conditions, can be simplified to a single degree of freedom roll motion depending on pitch and heave motions to be used in simulation studies (Newman, 1977; Milgram, 2003; Vanden Berg, 1991). Before the real-time an advanced active fin system control performance evaluations, necessary simulation studies were carried out by utilizing experimental data to obtain hydrodynamic coefficients and other ship dynamic characteristics from full-scale measurement tests on Marti (Ertogan, et al., 2016). The equation of a single degree of freedom roll motion depending on pitch and heave motions is given as (1).

$$(I + A)\ddot{\emptyset}(t) + \left(\frac{B_1 T_{\emptyset} \Delta\overline{GM}(t)}{\pi^2}\right)\dot{\emptyset}(t) + \left(\frac{B_2 3T_{\emptyset}^2 \Delta\overline{GM}(t)}{16\pi^2}\right)\dot{\emptyset}(t)\left|\dot{\emptyset}(t)\right| + \left(\Delta\overline{GM}(t)\right)\emptyset(t) = M_{SW}(t) + M_C(t) \quad (1)$$

The definitions of symbols in (1) are as follows; $\emptyset$, the ship's roll angle around the longitudinal axis, I, mass moment of inertia, A, added mass moment of inertia, B_1, B_2, roll damping moment proportional to a ship roll velocity, $T_\emptyset$, natural roll frequency, Δ, ship displacement, $\overline{GM}$, righting moment arm, M_{SW}, moment of sea wave forces, and M_C, moment of an active fin system.

An inclining experiment was carried out to calculate the vertical center of gravity (VCG) for Marti. In order to find the damping coefficient, the fins were actuated in calm sea conditions to force Marti to start a rolling motion a variety of speeds. As soon as the fins were stopped, the ship's roll motion was recorded by using the tilt sensor. Natural period $T_\emptyset$ at every a ship's speed was calculated according to the records. The time history of the measured roll angles at 7 knot is given in Fig. 6. To find the damping characteristics of Marti, on the roll decay curve $\emptyset$, on the axis of abscissas, a tangent to the curve is drawn for each period. The decrement in $\emptyset, \delta\emptyset \approx -\frac{d\emptyset}{dn}$, values can be found by measuring the slopes of these tangent lines. The expression for the resulting damping is given in (2), and shown in Fig. 7. Since K_1 and K_2 coefficients are found, nonlinear damping moment coefficients, D and E in (3) can be calculated according to (4). This procedure was repeated for Marti at variable speeds (Sabuncu, 1993).

$$-\frac{d\emptyset}{dn} = K_1\emptyset + K_2\emptyset^2 \tag{2}$$

$$B\dot{\emptyset} = D\dot{\emptyset} + E\dot{\emptyset}^2 \tag{3}$$

$$D = \frac{\pi^2 K_1}{T_\emptyset \Delta \overline{GM}}\ ,\ E = \frac{16\pi^2 K_2}{3T_\emptyset^2 \Delta \overline{GM}} \tag{4}$$

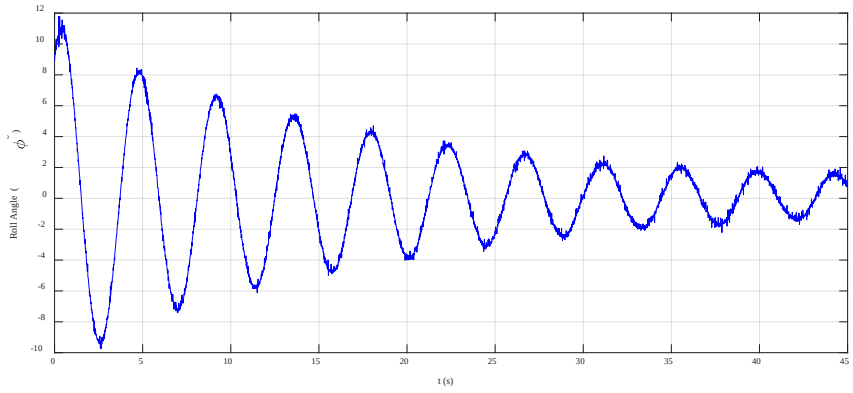

Fig. 6. Natural roll damping of Marti in calm sea condition.

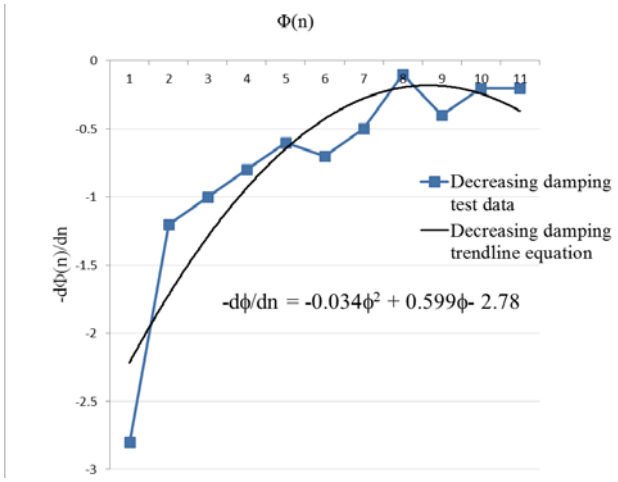

Fig. 7. Fitted curve of natural roll damping

Nonlinear restoring moment in (1) $\Delta\overline{GM}$, is calculated according to roll motion depending on heave and pitch motions by using Maxsurf-Hydromax^{TM} program. A sea spectrum was chosen according to the sea trial measurements such as roll, pitch motions, and heave motions, sea wave height, and wind speed by using Maxsurf-Seakeeping^{TM} program. In addition to these, the Froude-Krylov Hypothesis and diffraction moment methods were utilized for modelling the sea wave disturbance model and plugged into the right-hand-side of (1) M_{SW}. The high difference between one degree freedom roll motion depending on heave and pitch motions and one degree of freedom linear roll motion equations is shown on Fig. 8.

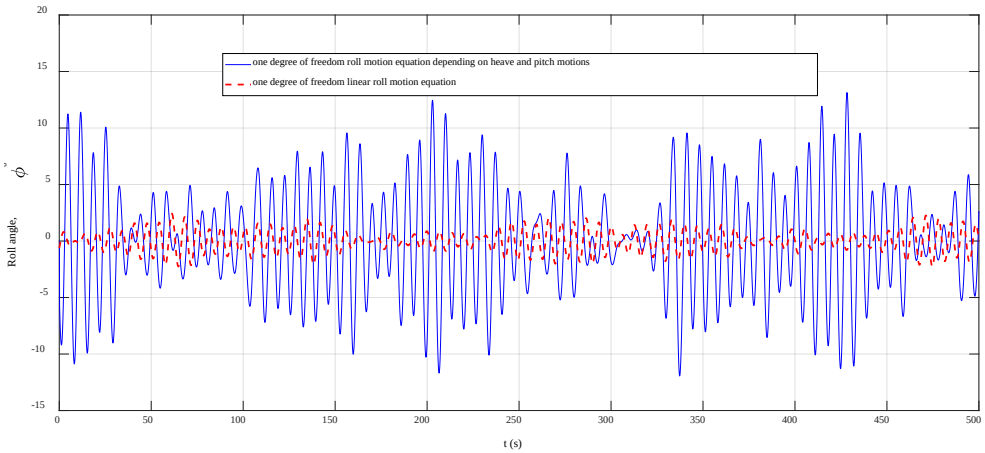

Fig. 8. Comparison of the linear and the nonlinear roll motion equations

In the second stage of the hydraulically actuated stabilizer fin system, a hydraulic control and fin-shaft mechanic systems were designed to be adapted a ship stabilizer system to each type of a ship. A hydraulic system was modelled as grey box method to be studied a hydraulic control system. A linear modelling of a hydraulic system can be used to obtain a system's delay and overshoot for controlling purposes. However, limits and capacities of hydraulic components

cannot be examined carefully with this approach. Due to this deficiency, a hydraulic system with ship roll motion, fins, and controllers was parametrically modelled. Every component can be changed and resized easily including ship, fins, hydraulic components and controllers with the help of the parametric modelling.

Hydraulic components including pump, accumulator, pressure relief valve, proportional valve, asymmetric cylinder, cylinder friction, and dynamical change of oil bulk modulus were modelled by combining catalogue data, bode diagrams, nonlinear equations. Full scale sea trials were made, after the hydraulic components were assembled on Volcano71. Then, collected experiment data was compared to simulation results. The nonlinear model also was used to solve some problems encountered in experiments. The problem was identified as fast reference alteration of roll controller caused by big roll angles according to high wave amplitudes. A reference signal, simulation, and experimental data are shown on Fig. 9. The simulation, and experimental data were obtained relatively close. In simulation environment, pump pressure and maximum flow were adjusted to find the reason for faulty traction. The possibility of inadequate pressure according to vessel speed was eliminated. To solve this, pump displacement was increased in simulation environment. The hydraulic system's response was accelerated and error was reduced with higher flow rates (Jelali and Kroll, 2003; Zihnioglu, et al., 2016).

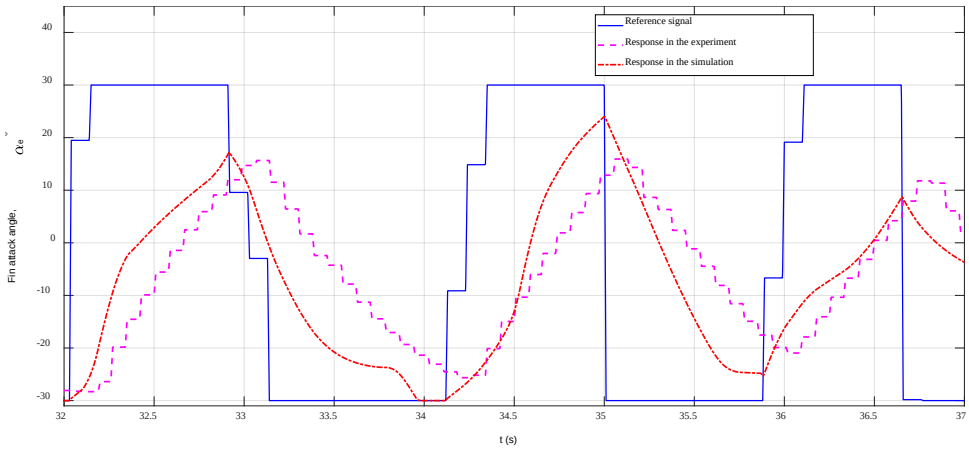

Fig. 9. The reference signal for fin attack angle, and the feedback signals from the potentiometers during the sea trials and simulation studies in severe sea wave condition (Zihnioglu, et al., 2016).

Another project was studied on optimal trim control of a high speed craft. The purpose of controller design can be to convert a manual trim system to an automatic controller, or to improve an existing controller. The mathematical model should represent the dynamic behaviour of a high speed craft and be useful for these control applications. Nonlinear dynamic model of pitch and surge motions of a high-speed craft was studied as black box method by using sea trials' data so that an optimal trim controller could be designed based on the obtained nonlinear model. The purposes of dynamic trim control are fuel efficiency, safety, comfort of passenger in a vessel. Dynamic modelling of a high speed

craft was studied by system identification (SI) methods such as state-space, AutoRegressive eXogenous (ARX) and Neural Networks (NNs) methods with sea trial data of Volcano71. A part of the collecting experiment data in several sea conditions was used to train the model, another part of the experiment data was used to validate the model. The most accurate dynamic model of a high speed craft was obtained by using NN method in SI methods (Ertogan, et al., 2017).

Furthermore, another black box modelling was studied for an autonomous underwater vehicle (AUV). A fully actuated AUV named as Delphin2 was developed at the University of Southampton. Its particulars are defined in Philips, et al. (2009). Its actuators are a propeller, the two vertical and horizontal thrusters placed in its front and aft, and the tails placed on horizontal and vertical axes. The AUV's coupled depth-pitch motions was modelled by using the collecting test data. The tests were realized as hover and flight style operations for altitude (vertical distance from bottom of the tank) range between 0.3 m - 1 m, in Lamont Towing Tank belonging to the University of Southampton, approx. 1.0 m depth, 2 m width, and 30 m length. The flight style operations were repeated for low, medium, and high speeds as the propeller's control signals at 10, 16, 22 (approx. 0.42 m/s, 0.82 m/s, 1.03 m/s).

The coupled depth and pitch motions of the AUV was modelled by using NN method. The inputs and outputs are illustrated on Fig. 10. Altitude values measured by an altimeter were used instead of depth (vertical distance from water surface) for the NN modelling. The past values' number of the outputs as 7, and the past values' number of the inputs as 5 were determined, so NN model with 34 inputs, and 2 outputs was used.

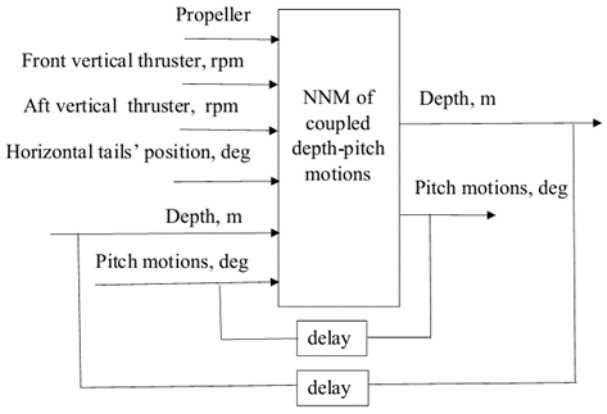

Fig. 10. The input and output signals for a dynamic model of depth-pitch motions of AUV.

This model includes two hidden layers. The neurons' number of the first, and the second hidden layers are the same as 7. As a result of practices, the log- sigmoid activation function for the first hidden layer, and the tan- sigmoid activation function for the second hidden layer were chosen, and the gradient descent with momentum and adaptive learning rate

backpropagation algorithm was used for training of the NN model. The training input, and output data for this model are shown in Fig. 11.

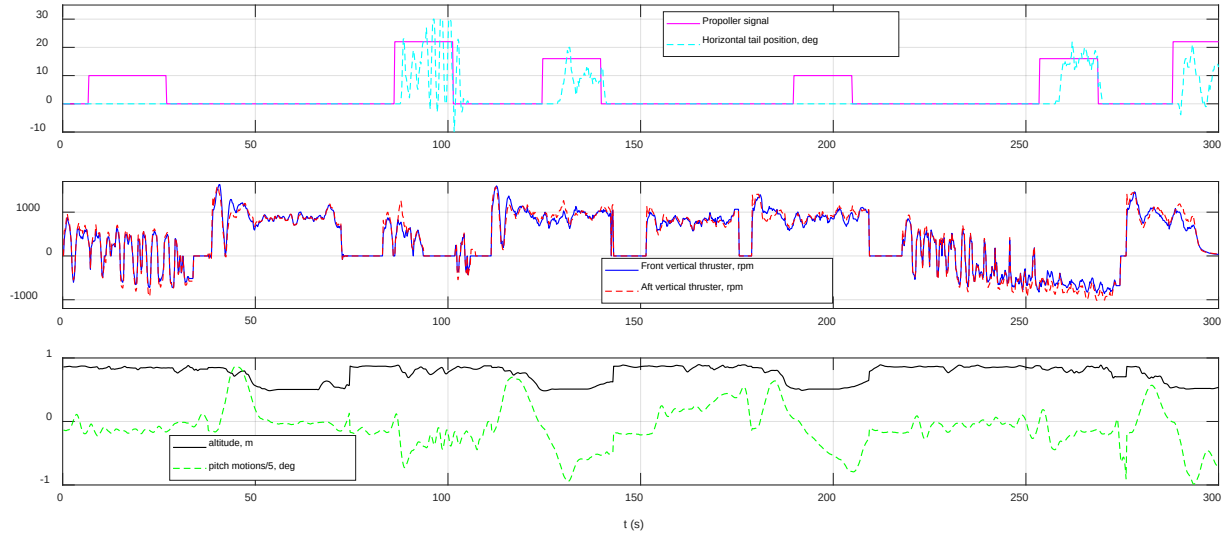

Fig. 11. Training input and output data for a coupled depth-pitch motions' ANN modelling

After the NN model was trained, it was validated by using test data. The comparisons between the NN model outputs and training, and validation data of depth, and pitch motions are shown in Fig. 12, and 13, respectively. Correlation coefficient (R), mean square error (mse), and normalized mean square error (nmse) values for the outputs of the depth-pitch motions NN model according to test data are given in Table 1.

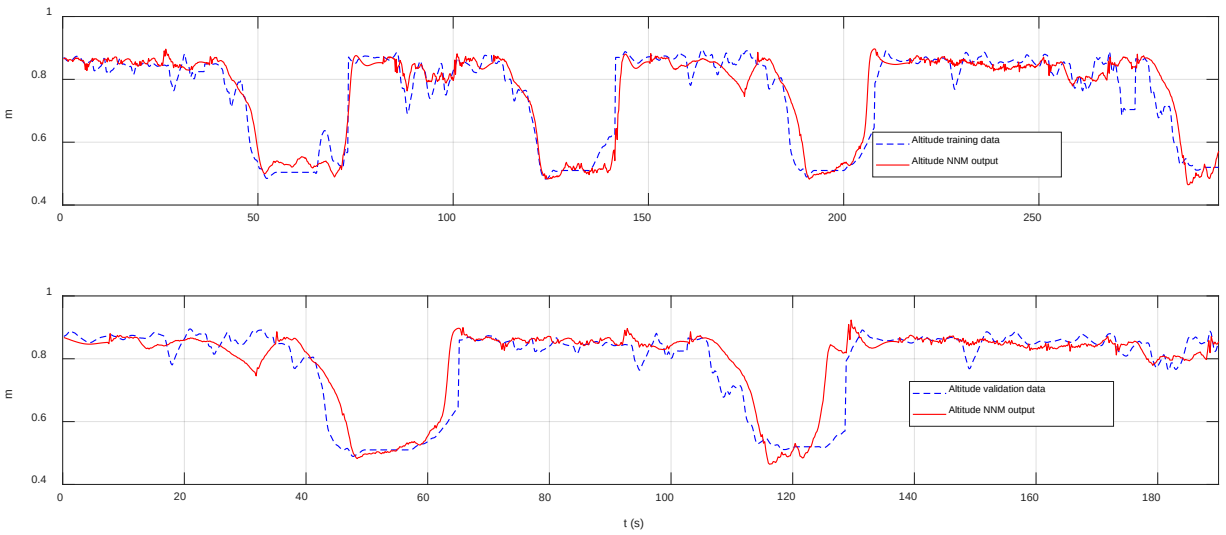

Fig. 12. Comparison between the NN model outputs and training, and validation data of depth motions

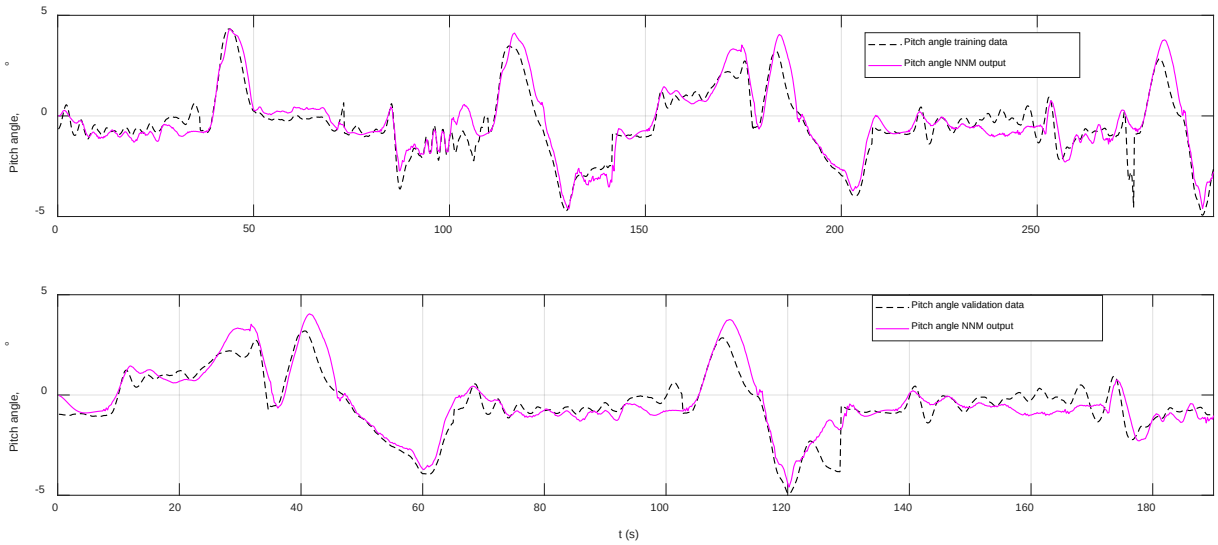

Fig. 13. Comparison between the NN model outputs and training, and validation data of pitch motions

Table 1: R, mse, and nmse values for the outputs of the depth-pitch motions NN model according to test data.

	Altitude, m		Pitch Angle, deg.	
	Training data	Validation data	Training data	Validation data
R	0.93	0.88	0.93	0.89
mse	0.003	0.004	0.429	0.508
nmse	0.85	0.75	0.84	0.77

4. Operations and control of marine mechatronic systems

Identifying measurement, actuator, and controller systems, setup and operation of mechatronic systems, controller tuning and performance evaluation are significant processes for real time control systems. These subjects are explained through the experiences on ship roll motion reduction hydraulically actuated control system, and trim control of a high speed craft in this section.

4.1 Operations of the marine mechatronic systems' prototypes

The drivers of the actuator systems can be chosen whether an open-loop controller or a closed-loop controller. An open control system is independent of a process output. It doesn't use feedback signal to determine for achieving a reference signal. A closed loop control system has feedback loop to correct any errors according to set value. The controller of the actuator needs to be programmed as cascaded in a main controller. For example, there are some options, such as a servo valve, a proportional valve, or on-off valve for the hydraulic valves in a ship roll motion reduction hydraulically actuated controller system. A servo valve has a closed-loop control for a cylinder's position control of a cylinder. A

proportional valve has an open-loop control. If a precision position control is essential for a mechatronic system, a closed-loop control can be programmed for a proportional valve with a position sensor such as LVDT. Furthermore, an on-off valve can be derived as proportional by Pulse-Width-Modulation (PWM) programming. A servo valve is the most expensive actuator in the hydraulic valves. An on-off valve has the least cost according to the other two actuator. A pair of servo valves were used in the ship roll motion reduction control system. The real-time closed-loop control block diagram of the hydraulic driven active fin system is shown in Fig. 14 (Ertogan, et al., 2016). The ship roll motion reduction controller sends fin attack angles, sent as reference to the hydraulic servo system, are measured using potentiometers placed on the system.

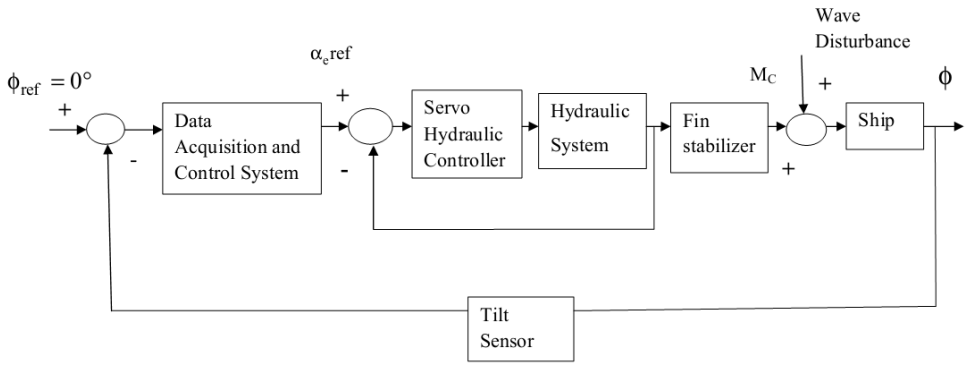

Fig. 14. The closed-loop control block diagram of the ship roll motion reduction system.

Furthermore, there are options for an actuator system, such as a hydraulic system with variable speed pump, or an electrical system for an actuator system of a stabilizer active fin system. A hydraulic system with variable speed pump does not need valve, and can be controlled by the pump. There is less energy loss in the system, because the flow rate in the system can be provided as needed. However, the closed-loop position control of the stabilizer fin system for variable pump hydraulic system is more difficult than the conventional hydraulic system. Although an electrical actuator system for the stabilizer fin system takes less space and less complex than the hydraulic system, it should be studied on capability of forward, and reverse rotations of an electric motor up to 1 Hz, or 2 Hz.

An active trim control of a high speed craft were actuated an interceptor, or a trim tab systems (Ertogan et al., 2015, 2017). An interceptor system needs less power than a trim tab system at the same dynamic force. In some applications, it may not possible to take feedback signal to drive the actuators, so the calibration process based on changing application areas is very important. An interceptor/trim tab systems are generally have electrical actuators and open-loop control drivers, so position calibration according to sending signals in sea condition states is significant before the control applications.

A ship's motion measurement system should be identified according to a project' requirements and budget. In the first stage of the ship roll motion reduction control project, 2D-tilt sensor was used, so roll and pitch motions of the ship could be measured. Velocities and accelerations of these motions were calculated by using the derivative and filtering methods which are explained in Section 4.2.

As a controller system, an embedded computer system may preferred for rapid prototyping of a marine mechatronic system, so a designed control algorithm can be programmed easier with a high-level program language. In real marine applications, PLC systems are generally preferred because of uninterrupted working and having the required certifications.

An analog electronic card might be preferred for the systems requiring classic Proportional-Integrative-Derivative (PID) controllers because of its rapid respond time, variety and simplicity (O'Dwyer, 2009). The PID analog drivers were used for the hydraulic system of the ship roll motion reduction active fin system. The more complexity a system has, the higher the specifications of its controller must have. However, the more capacity, and execution time they have, the higher cost they have. So, an industrial electronic card including a microcontroller should be produced in series production of a marine equipment because of its cost efficiency. Although it has a high cost in the first certification process, its cost will be reduced in its series production.

4.2 Measurement, noise, derivative problems, and filtering methods

In real-time, closed-loop control applications, there are problems such as noisy measurements and derivative processes. Butterworth filters are frequency based digital filters. The common problem encountered in using Butterworth filters is the phase delay problem (Butterworth, 1930). The comparison between the averaging filter and first-order low pass Butterworth filter applications on noisy roll angle measurement is shown in Fig. 15. The decision should be made that the phase delay problem can be tolerated, or not, according to a sensor's signal output frequency range, and the closed-loop time of an application.

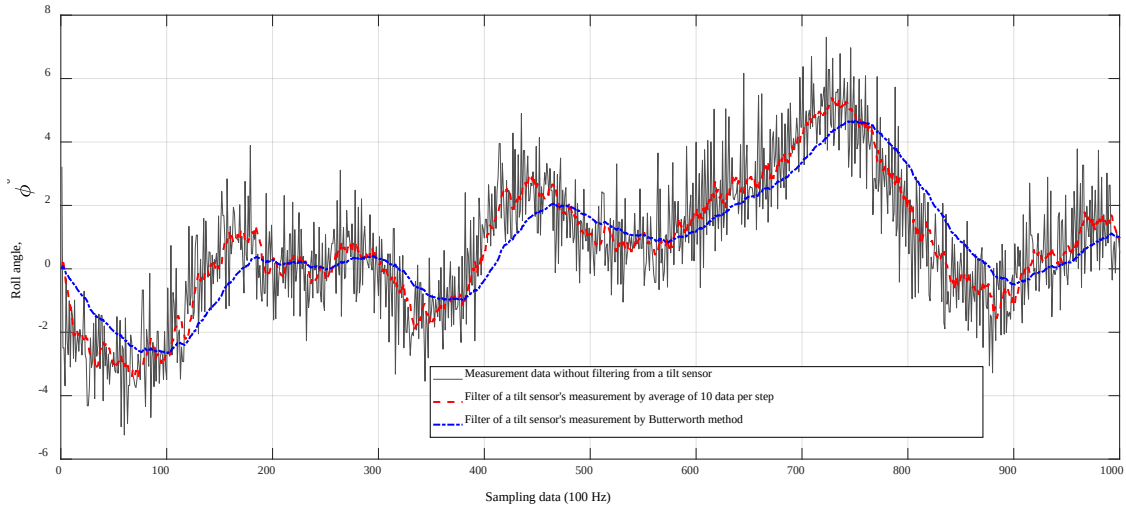

Fig. 15. Comparison of filtering methods for noisy measurement data

Also, derivation of the position signal data may be required, either to reduce feedback signals, or doesn't have an alternative sensor for measuring velocity. A general derivative process is the Euler method, but this method may not give accurate results. An efficient velocity estimation algorithm is Enhanced Differentiator (ED) (Su, et al., 2006). Also, ED method can be used for filtering noisy signal data. For this velocity estimation application, ED method is given in (5) and (6). $\hat{p}$ and $\hat{v}$ represent the estimated position and velocity, respectively. $\varepsilon(k) = \hat{p}(k) - p(k)$ is the position estimation error. p is the reference position, T is the sampling period, and k denotes the kth sampling instant. $\alpha_0, \alpha_1, \alpha_2, R, n, m$ are design parameters (Su, et al., 2006). In addition to this, K_t, a constant, tuned according to a sensor's sampling time, was added in (5) and (6). For example, if sampling time is 0.01, or 0.05 s, K_t should be tuned 10, or 50 respectively. Also, $\hat{p}$ and $\hat{v}$, the estimated position and velocity data are complex numbers. The comparison of the roll velocity measured by a gyro, and the velocity estimation by ED method based on the roll angle measurement with a tilt sensor is shown in Fig. 16. The ED method estimates the roll velocity successfully. However, the design parameters need to be tuned differently for offline and real time applications.

$$\hat{p}(k+1) = \hat{p}(k) + \left(\frac{T}{K_t}\right)\hat{v}(k) \tag{5}$$

$$\hat{v}(k+1) = \hat{v}(k) + (T/K_t)R^2\left[-\alpha_0\varepsilon(k) - \alpha_1\left(\varepsilon(k)\right)^{n/m} - \alpha_2\left(\frac{\hat{v}(k)}{R}\right)^{n/m}\right] \tag{6}$$

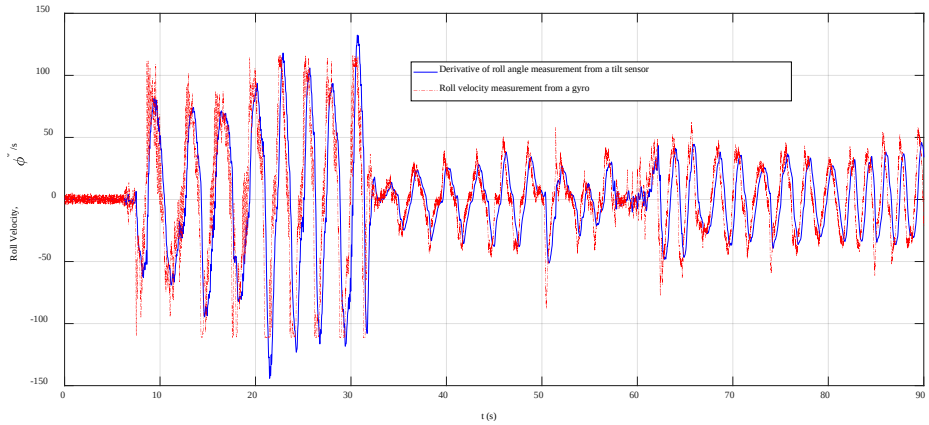

Fig. 16. Application an ED derivative method using a tilt sensor's data.

Furthermore, the complementary filter (CF) method (Mahony, et al., 2008) was applied for a low-cost IMU sensor, MinIMU-9-v2^{TM}. Its simple form equation is given in (7). Every iteration, the Euler angle values are updated with the new gyroscope values by taking 98% of the current value, and adding 2% of the angle calculated by the accelerometer. The constants, 0.98 and 0.02 have to add up to 1, and they may be changed to tune the filter properly. The implementation of the CF is easier than Kalman Filter (KF), but the CF has to applied in high frequency. The pitch angle outputs of the low-cost sensor with the CF and Microstrain 3DM-GX4-45^{TM} used as reference signal are shown in Fig. 17. For 50 Hz application, nmse, 83%, mse, 1.62° were calculated.

$$\text{Euler angle}=0.98*(\text{Euler angle}+\text{gyro\_data}*dt)+0.02*(\text{acceleration\_data}) \quad (7)$$

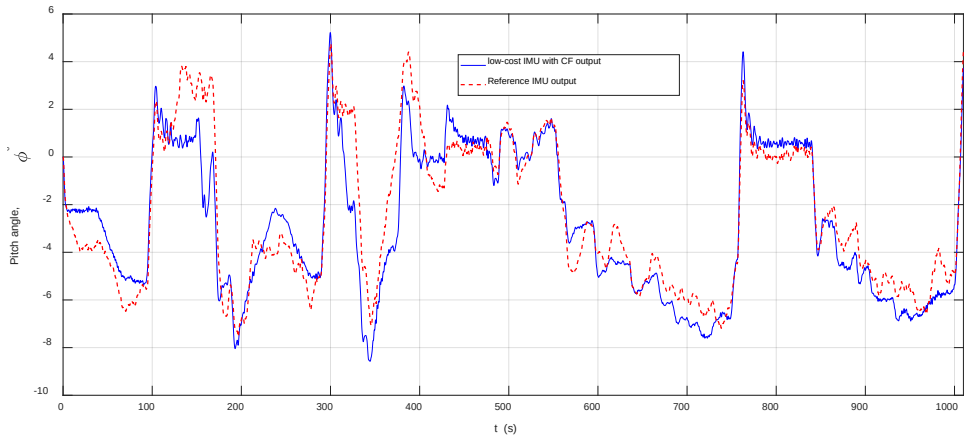

Fig. 17. The CF application for the low-cost IMU sensor, and comparison to the referenced IMU including the KF.

4.3 Controller tuning and performance evaluation

Determination of state variables, signal output frequency of feedback sensors, and closed-loop control signal time are main important issues. Impact of each variable, sample time, and control signal time must be defined by real time

applications. Controller coefficients of a classic controller, or range of controller coefficients for an advanced controller must tuned according to full scale experiments. These issues are explained through the implemented projects.

The efficient state variables roll motion angle, roll velocity and acceleration were determined for the ship roll motion reduction control. It can be seen from the literature survey that the most common ship roll damping controller is Proportional-Derivative-Second Derivative (PDD^2) using roll amplitude, roll velocity and acceleration variables. This was also verified by simulations, and full-scale experiments during the study. Increasing the control coefficient K_p of PDD^2 controller shows the influence of increasing the ship's metacentric height $\overline{GM}$. So, the coefficient K_p is effective in reducing the rolling period of the ship. Reducing the amplitude of the roll motion depends on K_d which is the coefficient of the roll velocity error. The roll acceleration coefficient, K_{d^2}, increases the roll period. K_{d^2} coefficient is effective in reducing a ship's $\overline{GM}$. If there isn't the possibility to do an inclining experiment, a ship's $\overline{GM}$ may be calculated according to an empirical equation in (8) where *C* is a constant, approximately equal to 0.40 for merchant ships, *B* is the width expressed in feet, and $\overline{GM}$ is expressed in feet. Natural roll period time series data, $T_\emptyset$ is measured in calm sea at zero speed (Burger and Corbet, 1966).

$$T_\emptyset = \frac{C*B}{\sqrt{\overline{GM}}} \tag{8}$$

The performance efficiency of a ship's roll motion reduction with an active fin system was evaluated according to the total percentage damping ratio, ρ and the statistical roll motion reduction constant, F. The total percentage of roll motion reduction, ρ describes the decrease in the overall degree of stabilized motion compared with that of unstabilized motion. As a general method for the performance evaluation of the percentage of roll motion damping ratio, shown as ρ, is given in (9). One of PDD^2 controller applications with PLC on Volcano 71 is shown in Fig. 18, while the controller was open and closed, respectively. PDD^2 control was provide %76 roll motion reduction.$\rho[\%] = 100 *$

$$\left(1 - \frac{stabilized\ roll\ angles}{unstabilized\ roll\ angles}\right) \tag{9}$$

In this calculation, the total roll motion reduction ratio is evaluated as total roll angles; however, it does not make any distinction between small and large roll angles in terms of proportions. The statistical roll motion reduction constant (F), allows one to distinguish between small and large roll angles. The higher F constant is, the better the performance the stabilizer controller has (Krosys, 2010).

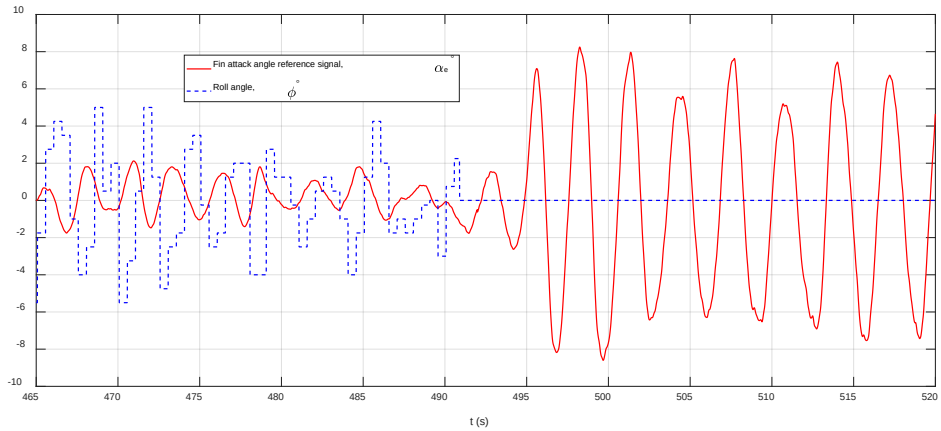

Fig. 18. Roll motion was measured while PDD[2] control was on and off respectively, on Volcano 71, in the sea trials.

The cumulative probability of exceeding a given roll angle, x, is calculated with the Rayleigh Distribution as $e^{\left[-x^2/2m_0\right]}$ where m_0 is the mean square value of roll angles. The area under the spectrum of stabilized and unstabilized roll angles is calculated with equations $e^{\left[-x^2/2m_{0s}\right]}$ and $e^{\left[-x^2/2m_{0u}\right]}$ respectively. Then F coefficient is given in (10).

$$\frac{e^{\left[-x^2/2m_{0s}\right]}}{e^{\left[-x^2/2m_{0u}\right]}} = e^{\left[-Fx^2\right]},\ F = \frac{1}{2m_{0s}}\left(1 - \frac{2m_{0s}}{2m_{0u}}\right) \tag{10}$$

The percent damping ratio ζ depending on F coefficient for any given roll angle x is calculated as in (11).

$$\zeta[\%] = \left(1 - e^{(-F*x^2)}\right) * 100 \tag{11}$$

By using (11), a better distinction can be made between small and large roll angles' damping. Thus, the performance of the active fin controller can be evaluated in more detail. For example; damping ratios for exceeding each roll angle can be calculated when F damping coefficient values are 0.03 and 0.04. For a stabilizer giving F=0.03, the number of rolls greater than 5° is reduced by 53%. If F is increased 0.04, the reduction will be 63%.

For the comfort of passengers and crew members of ships, inertial forces caused by ship motion must remain under certain limit values. For example, if the heave acceleration exceeds 1/10 of gravitational acceleration, passengers and crew experience the symptoms of seasickness. (12) is given between the roll amplitude and the roll acceleration with the assumption of a simple harmonic roll motion to analyse the heave acceleration (Newman, 1977; Sabuncu, 1993). Due to the requirement of $\ddot{z} \leq 0.1g$, the largest angular displacement for the roll acceleration is calculated using (13). For example, Marti's beam is taken as B=4.5 m for the calculations. $\emptyset_a$, the largest angular displacement of roll motion and $\omega_\emptyset$, the angular frequency of roll motion are determined. $T_\emptyset$, is the natural roll period in calm sea

conditions and measured for Marti as 4 seconds. Hence, the maximum amplitude of roll acceleration was calculated as $10\,°/s^2$.

$$\ddot{z} = \frac{B}{2}\ddot{\emptyset} = \frac{B}{2}\emptyset_a \omega_{\emptyset}^2 \tag{12}$$

$$\emptyset_a \leq 0.1g\left(\frac{T_{\emptyset}}{2\pi}\right)^2 \frac{2}{B} \tag{13}$$

The fin attack angle and angular velocity must not exceed the saturation values for the active fin stabilizer system to work efficiently. Mechanically, the fin attack angle must be within maximum of $\alpha_{emax} = \mp 30^{\circ}$. The maximum fin attack angular velocity may be applied as $\dot{\alpha}_{emax} = \mp 30\,°/s$ .However, the saturation value of the fin attack angle velocity varies with hydrodynamic effects depending on the speed of the ship and sea conditions, so the maximum fin attack angular velocity should be changed as nonlinear.

In another project as optimum trim control, after the installation of an interceptor, and a trim tab systems on Volcano 71, the systems were operated manually in several sea conditions, shown in Fig. 19, for system identification purposes, and determining sampling time, and response time.

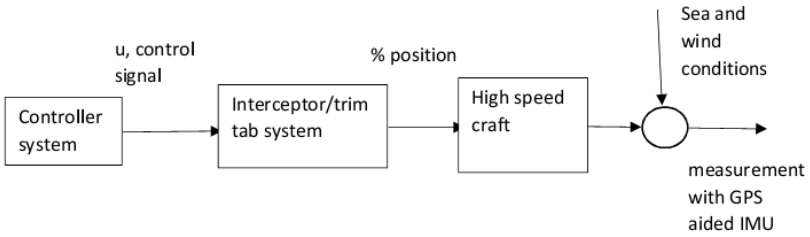

Fig. 19. Manual control of the interceptor/trim tab system

The positions of the interceptor, and trim tab systems were open loop controlled, and they were operated separately. The control time of the interceptor/trim tab system was implemented as 3 s, and 5 s, because a GPS' delay response time as 2-3 s was taken into account, for first its manual control applications during sea trials, and the sample time for the GPS aided IMU sensor was implemented as 0.1 s. However, it was determined that the control period had to be longer such as 20 s after many applications. The sampling time wasn't be changed because the GPS aided IMU' data was used for the modelling, and required to be filtered. The results of the sea trials have been proved that an optimum position of the interceptor/trim tab system should be changed as automatically to obtain maximum a ship's speed at constant an engine power according to changing environmental conditions. The sample of the applications is shown in Fig. 20.

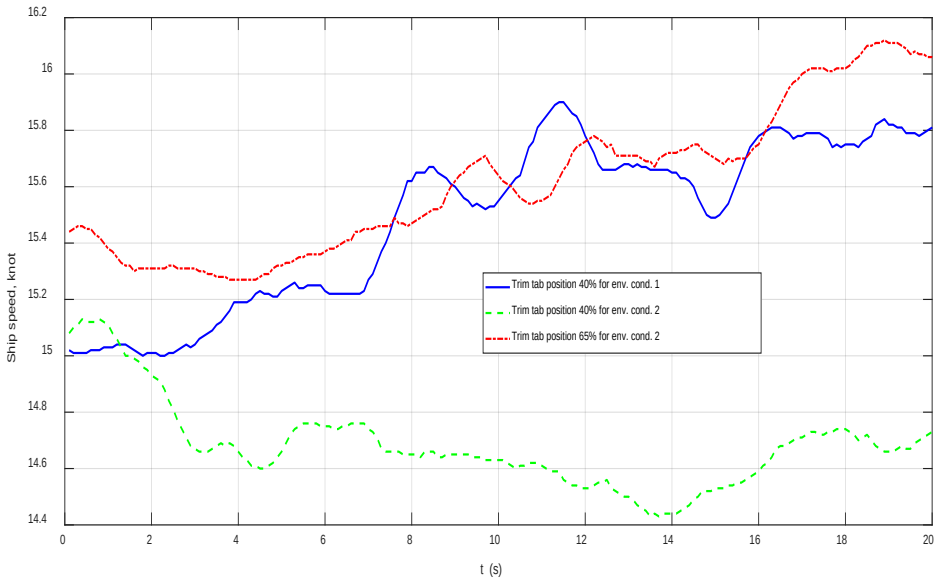

Fig. 20. Responses of the trim tab positions, 40%, and 65% at constant an engine power during changing environmental conditions

5. Conclusions and future works

In this paper, the definition of ship motion modelling according to control applications, the methods of data acquisition, signal processing and filtering, the particulars of the controllers, the sensors and the features of the communication types were reviewed. The presented modelling, and signal conditioning methods for marine control systems were proved by the case studies. Furthermore, the required characteristics of marine control systems such as sampling time, closed loop control time, identification of model, and control parameters were defined based on the experiences of the realized projects. Also, the applied methods of controller tuning and performance evaluation were presented. In addition to these, insight into the selection of hardware and software components for mechatronic applications in marine engineering was provided.

Nonlinear grey box method applications on ship roll motion, a hydraulic system of a ship roll motion reduction control system, and Neural Network (NN) modelling for a coupled pitch-surge motions of a high speed craft were presented as the case studies. Also, NN modelling for coupled depth-pitch motions of a fully actuated AUV was applied, and obtained high fitting ratios.

For measurement process, an efficient velocity estimation method, Enhanced Differentiator (ED) was applied, and obtained good results according to a referenced gyro sensor. Also, Complementary Filter (CF) method was implemented for a low-cost IMU sensor, compared to a referenced IMU sensor including Kalman Filter code. As a

result of this application, nearly good enough fitting ratio was obtained. The CF application frequency may be increase to increase performance.

The ongoing projects are as follows: Pitch-heave motion reduction control system of a high speed craft is currently studied as a continuation of optimal automatic trim control system. Also, the turning radius can be keep smaller and safe during manoeuvres in several speed and sea conditions by using an interceptor or stern driving system of a high speed craft. The collecting data with sea trials is ongoing for two applications. In addition to these, dynamic position control of AUVs is carried on as theoretical and practical studies. Furthermore, the ride control which involves both pitch and roll motion control for high speed vessels will be studied in the future.

Acknowledgments

The authors would like to thank the Republic of Turkey Ministry of Industry and Trade entrepreneurs fund for the support provided for the project numbered 0067.TGS.2009. The authors would also like to thank I.T.U. Scientific Research Funds for the project numbered 37491 with the partial support. Furthermore, the authors would like to thank The Scientific and Technological Research Council of Turkey for the 7120809, 7141282, 1059B191501331 numbered projects' support.

7. References

Ahmed, N., Ghazilla, R.A.R., Khairi, N.M., 2013. Reviews on various inertial measurement unit (IMU) sensor applications. International Journal of Signal Processing Systems, Vol. 1, No. 2, pp. 256-214.

Bandara, D., Leong, Z., Nguyen, H., Jayasinghe,S., Forrest, A.L., 2016. Technologies for underwater-ice AUV navigation. IEEE/OES, Autonomous Underwater Vehicles (AUV), Tokyo, Japan,

Burger, W., Corbet, A.G., 1966. Ship Stabilizer, First Edition, Pergamon Press Ltd., Headington Hill Hall, Oxford, London, England.

Butterworth, S., 1930. On the theory of filter amplifiers. Experimental wireless & the wireless engineer, pp. 536-541.

Cain, C., Leonessa, A., 2012, "Laser based rangefinder for underwater applications", American Control Conference, Canada, pp. 6190-6191.

Chong-Moo Lee, Pan-Mook Lee, Seok-Won Hong, Sea-Moon Kim, 2005. Underwater navigation system based on inertial sensor and doppler velocity log using indirect feedback Kalman Filter. International Journal of Offshore and Polar Engineering, Vol. 15, No. 2, p. 8895.

Ertogan, M., Tayyar, G.T., Karakas, S., Ertugrul, S., 2015. Review of measurement and real-time control systems for marine applications", The 4th International Conference on Advanced Model Measurement Technologies for the Maritime Industry, AMT'15, Istanbul, Turkey.

Ertogan, M., Ertugrul, S., Taylan, M., 2016. Application of particle swarm optimized PDD^2 control for ship roll motion with active fins. IEEE-ASME Transactions on Mechatronics, Vol. 21, Issue: 2, pp. 1004-1014.

Ertogan, M., Wilson, P.A., Tayyar, G.T., Ertugrul, S., 2017. Optimal trim control of a high-speed craft by trim tabs/interceptors Part I: Pitch and surge coupled dynamic modelling using sea trial data. Ocean Engineering, Vol. 130, pp. 300-309.

Jelali, M., & Kroll, A., 2003. Hydraulic servo-systems: modelling, identification and control. Springer.

Karras, G.C., Loizou, S.G., Kyriakopoulos, K.J., 2011. Towards semi-autonomous operation of under-actuated underwater vehicles: sensor fusion, on-line identification and visual servo control. Autonomous Robots, Volume 31, Issue 1, pp. 67-86.

Knezic, M., Ivanovic, Z., 2013. Evaluation of Ethernet over EtherCAT Protocol Efficiency. INFOTEH-JAHORINA, Vol. 12.

Ljung, L., 1999. System identification: theory for the user. Prentice Hall, Second Edition.

Mahony, R., Hamel, T., Pflimlin, J.M., 2008. Nonlinear complementary filters on the special orthogonal group. IEEE Transactions on Automatic control, Vol. 53, No. 5, pp. 1203-1218.

Milgram, J.H., 2003. Numerical methods in incompressible fluid mechanics. Lecture Notes, MIT, USA.

Newman, J.N., 1977. Marine Hydrodynamics, The MIT Press Cambridge, Massachusetts, and London, England.

O'Dwyer, A., 2009. Handbook of PI and PID controller tuning rules. 3rd edition, Imperial College Press., London.

Paull, L., Saeedi, S., Seto, M., Howard Li, 2014. AUV navigation and localization: a review. IEEE Journal of Oceanic Engineering, Vol. 39, No. 1, pp. 131-149.

Perez, T., Blanke, M., 2002. Mathematical ship modelling for control applications. Technical Report.

Philips, A.B., Steenson, L., Harris, C., Rogers, E., Turnock, S.R., Furlong, M., 2009. Delphin2: An over actuated autonomous underwater vehicle for manoeuvring research. Trans. RINA, International Journal Maritime Engineering, Vol. 151, Part A1, pp.

Plueddemann, A.J., Kukulya, A.L., Stokey, R., Freitag, L., 2012. Autonomous underwater vehicle operations beneath coastal sea ice. IEEE/ASME Transactions on Mechatronics, Vol:17, Issue:1, pp. 54-64.

Sabuncu, T., 1993. Ship Motions, Faculty of Naval Architecture and Ocean Engineering, Istanbul Technical University, Turkey.

Su, Y.X., Zheng, C.H., Mueller, P.C., Duan, B.Y., 2006. A simple improved velocity estimation for low-speed regions based on position measurements only. IEEE Transactions on Control Systems Technology, Vol. 14, No. 5, pp. 937-942.

Talbot, S.C., Ren, S., 2009. Comparison of FieldBus systems, CAN, TTCAN, FlexRay and LIN in passenger vehicles. 29th IEEE International Conference on Distributed Computing Systems Workshops.

Tetley, L., Calcutt, D., 2001. Electronic navigation system. 3rd edition, Butterworth-Heinemann, Oxford, a division of Reed Educational and Professional Publishing Ltd.

Valesco, F. J., Herrero, E.R., Lopez, E., Moyano, E., 2013. Identification for a heading autopilot of an autonomous in-scale fast ferry. IEEE Journal of Oceanic Engineering, Vol. 38, No. 2, pp. 263-273.

Vanden Berg, S.M., 1991. Non-linear of ships in large sea waves. M.S. thesis, MIT, USA.

Xiang, X., Yu, C., Zhang, Q., 2017. On intelligent risk analysis and critical decision of underwater robotic vehicle. Ocean Engineering, Vol. 140, pp. 453-465.

Xiang, X., Lapierre, L., Jouvencel, B., 2015. Smooth transition of AUV motion control: From fully-actuated to under-actuated configuration. Robotics and Autonomous Systems, Vol. 67, pp. 14-22.

Zihnioglu, A., Ertogan, M., Tayyar, G.T., Karakaş, C.S., Ertugrul, S., 2016. Modelling, simulation and controller design for hydraulically actuated ship fin stabilizer systems. The 3rd International Conference on Control, Mechatronics and Automation, ICCMA, Vol. 42.

Bachmann. 2015. Manual for Maritime application – integrated automation systems. http://www.bachmann.info/fileadmin/media/Service/Downloads/Branchenbroschueren/BB_maritime.application_052014_EN_web.pdf (accessed 11.05.2015)

Djiev, S., 2015. Industrial networks for communication and control. http://anp.tu-sofia.bg/djiev/PDF%20files/Industrial%20Networks.pdf (accessed 02.05.2015)

Krosys. Technical Manual for Fin Stabilization System by Krosys Inc. http://www.krosys.com/pdf/fin/fin-technic.pdf (accessed 2010)

Servo2go. Comparing CANopen and EtherCAT FieldBus Networks. 2013. Technical support information. https://servo2go.wordpress.com/2013/09/23/comparing-canopen-and-ethercat-fieldbus-networks/ (accessed 13.09.2013)